JACS
JOURNAL OF THE AMERICAN CHEMICAL SOCIETY
Communication
pubs.acs.org/JACS

Multifluorescently Traceable Nanoparticle by a Single-Wavelength Excitation with Color-Related Drug Release Performance

Deli Lu, Juying Lei, Lingzhi Wang,* and Jinlong Zhang*

Key Lab for Advanced Materials and Institute of Fine Chemicals, East China University of Science and Technology, 130 Meilong Road, Shanghai 200237, P. R. China

Supporting Information

ABSTRACT: Monodisperse and nanometer-sized periodic mesoporous organosilicas co-doped with fluorescence resonance energy transfer cascades composed of triple fluorophores at various ratios were prepared. These nanoparticles exhibit multifluorescent emissions by a single-wavelength excitation and were designed for the application as multichannelly traceable drug carriers. Different from the hydrophilic framework of inorganic mesoporous silica and hydrophobic framework of mesoporous carbon, these multifluorescent nanoparticles have intrinsically different and finely tunable pore surface polarities governed by the type and amount of fluorophore inside the framework. When applied as drug carriers, they can achieve synchronous or asynchronous release of different drugs by simply choosing different colored nanoparticles. These colorful mesoporous composites with finely tunable color-related drug release performance provide a strong barcoding system for the potential applications of fluorescent nanoparticles in effective screening of drugs and therapeutic protocols for diseases.

The determination of an optimum therapeutic protocol for diseases, especially for the combinational drug administration protocol, is based on the abundant information about drug category, administration route, and releasing rate, among other things, which requires the use of a strong barcoding system for the effective sieving of drugs. Recently, fluorescent mesoporous silica nanoparticles (NPs) assembling abundant mesopore and fluorescence in a single nanoparticle (NP) have been intensively studied as fluorescently traceable drug delivery vehicles, which provide a good platform for the simultaneous drug delivery and real-time monitoring of the biodistribution of NPs after their entering into a biosystem.[1−8] However, the fluorescence emission of the current drug carrier generally lacks modulability. The introduction of fluorescence resonance energy transfer (FRET) tandem into an appropriate silica base can lead to the improved FRET efficiency and the formation of colorful NPs.[9,10] Unfortunately, for the application as biomarkers in high-throughput drug screening, the surface property of mesoporous NP still seems too monotonous to be worth the abundant fluorescent colors, although it can be modified with various functional groups through direct or post treatment.[11−13] Moreover, the pore surface functionalization and the introduction of fluorescent tags to the mesoporous channel easily lead to the pore blockage. Therefore, it is extremely desirable to design a novel mesoporous NP with tunable fluorescence and intrinsically different pore surface polarities, which should be directly and actively correlated.

Here, we present the successful synthesis of nanometer-sized and monodisperse fluorescent periodic mesoporous organosilica (PMO) simultaneously embedded with three kinds of fluorophores at various ratios inside the framework, which exhibits abundant colors by a single-wavelength excitation and has unimpeded pore channel without the blockage by fluorescent tags. Although PMO composites doped with various groups including large-sized fluorophore have been reported,[14−16] there is still no report on the synthesis of fluorescent and nanometer-sized NP with good monodispersity. The current lack of monodisperse fluorescent PMO NP has greatly restricted its bioapplication, which should be ascribed to the difficulty in the morphology control when introducing large-sized fluorophore into the thin framework wall due to the extremely fast hydrolysis rate of bis-silane. Moreover, PMO NPs present here exhibit color-determinative affinity to drug molecules when applied as drug carriers, which means the release performance of drug molecules can be tuned by simply choosing NPs with different colors. In a word, the importance of this communication lies in that it is the first report of multifluorescent PMO NPs with unique color-related release performance for drug molecules.

The successful fabrication of multifluorescent PMO NP here is achieved using a modified and mild Stöber system (see Supporting Information). The multicolor emission by a single-wavelength excitation results from FRET between different dyes. Here, bis-silylated biphenyl (Biph), anthracene (Anth), and naphthalimide (Naph) are chosen for the building of FRET cascades, which play the roles of energy donor, intermediate, and terminal acceptor, respectively. The preparation of bridged organosilane precursors $(R'O)_3Si\text{-}R\text{-}Si(OR')_3$ is through the reaction between fluorophore and 3-aminopropyltriethoxysilane (APTS, Scheme 1). The choice of dyes is due to good overlaps between the emission spectra of energy donor and the excitation spectra of acceptor required by FRET (Figure S1).

The influence of doping amount to the fluorescence property of PMO NP was first investigated by choosing Biph doped samples as models. As seen from Figure 1A, samples prepared by co-condensation of tetraethyl orthosilicate (TEOS) and bis-silylated Biph show maximum emissions at 320 nm, which first increase with the decreasing TEOS/Biph from 20 to 10, and

Received: February 20, 2012
Published: May 16, 2012

dx.doi.org/10.1021/ja301691j | J. Am. Chem. Soc. 2012, 134, 8746−8749

Scheme 1. Synthesis Routes for Bis-silanes

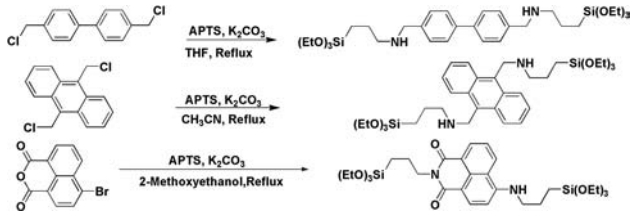

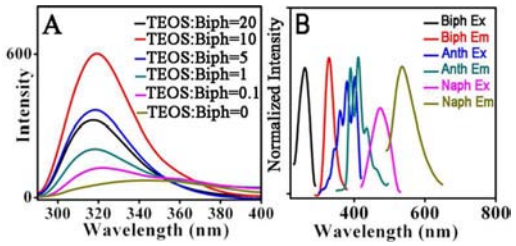

Figure 1. (A) Fluorescence emissions of Biph doped PMO solution (50 μg/mL). (B) Excitation and emission spectra of PMO doped with Biph, Anth, or Naph (TEOS/bis-silane = 10).

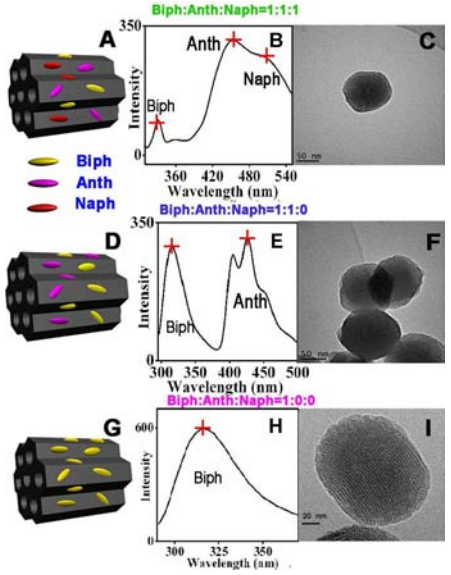

Figure 2. Illustrations (A, D, and G), emission spectra (B, E, and H), and TEM images (C, F, and I) of PMO co-doped with triple-dye at various ratios (TEOS/bis-silane = 10): (A–C) Biph/Anth/Naph = 1:1:1; (D–F) Biph/Anth/Naph = 1:1:0; and (G–I) Biph/Anth/Naph = 1:0:0.

then gradually decrease with the further decreasing of TEOS/Biph to 0.1. Moreover, sample prepared with 100% Biph shows a weak and red-shifted emission at 350 nm, indicating the self-quenching of fluorescence and decreasing of the transition energy caused by the high conjugation of dye molecules. All of samples show a spherical shape as seen from SEM images (Figure S4). Moreover, samples prepared at TEOS/Biph $\geq$ 1 show good hydrophilicity, which all form stable colloidal suspensions in water (Figure S5). More introduction of Biph makes samples less hydrophilic and decreases the dispersibility in water. On the basis of the above results, the fluorescence performance of samples doped with different fluorophores were further studied by fixing TEOS/bis-silane = 10. Figure 1B shows that the single introduction of Biph, Anth, or Naph does not change the excitation and emission spectra, where the emission spectra of energy donor and the excitation spectra of energy acceptor still have good overlaps.

Subsequently, the tunable fluorescence property of triple-dye doped PMO NPs was studied by varying the ratio between FRET tandems. Figure 2B shows that PMO NPs co-doped with triple dyes at an equal ratio simultaneously shows three peaks centered at 320, 460, and 520 nm by using the maximum absorption wavelength of Biph at 280 nm, which are attributed to the emissions of Biph, Anth, and Naph, respectively. For comparison, sample co-doped with Biph and Anth at an equal ratio (Figure 2E) only shows the emission of Biph at 320 nm and three adjacent peaks ranging from 400 to 450 nm attributed to Anth. Sample only doped with Biph (Figure 2H) shows a single emission at 320 nm. To illustrate the existence of FRET between different fluorophores, samples singly doped with Naph and co-doped with Anth and Naph are also excited at 280 nm (samples a and b, Figure S6A). Although emissions from Anth and Naph are still observable since all of fluorochromes containing phenyl group have absorption in UV range due to $\pi \rightarrow \pi^*$ transition, they are much improved in triple-dye doped sample due to the FRET from Biph to Anth and subsequently to Naph. The FRET can be better illustrated by exciting samples a and b using the maximum absorption wavelength of Anth at 375 nm (Figure S6B), where sample b shows both emissions of Anth and Naph but sample a only shows a background level of fluorescent intensity since Naph has negligible absorption in this wavelength. The effective FRET in above samples results from the shortened distance between energy donor and acceptor in the nanometer-sized thick framework wall (Scheme 2). The above results well

Scheme 2. FRET between Triple Dyes by a Single-Wavelength Excitation

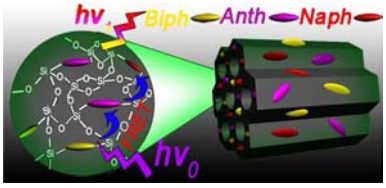

indicate the NP color can be finely tuned by varying the dopants ratio. Moreover, as seen from TEM images (Figure 2C,F,I), the introduction of Biph or Anth leads to the formation of NPs with similar size of about 140 nm, but the introduction of Naph leads to the decreased size of about 90 nm. All of PMO NPs doped with single, dual, and even triple fluorophores have good monodispersity. These NPs also have similar BET surface area (500 m^2/g) and average pore size (2.5 nm) (Figures S7–S9 and Table S1).

The arrangement of triple fluorophores inside the nanoscale-thick framework wall preserves the pore accessibility by isolating fluorophores from the pore channel and accelerates the FRET efficiency between energy donor and acceptor by shortening their distance. The advantage of such an arrangement is that drug molecules do not need to share space with fluorescent tags when these NPs are applied as drug carriers. Moreover, compared with hydrophilic framework of inorganic mesoporous silica and hydrophobic framework of mesoporous carbon, the inorganic–organic hybrid framework of the above multifluorescent mesoporous NPs should possess more tunable surface polarity due to the co-existence of hydrophobic

dx.doi.org/10.1021/ja301691j | J. Am. Chem. Soc. 2012, 134, 8746–8749

polycyclic fluorophore inside the framework and hydrophilic hydroxyls on the pore surface. Subsequently, we chose camptothecin (CPT), a commonly used anticancer drug as the model and studied the loading and releasing performance of PMO NPs prepared at TEOS/bis-silane = 10. Typically, the above three colored samples prepared at Biph/Anth/Naph = 1:0:0 (denoted as 100, similarly hereinafter), Biph/Anth/Naph = 1:1:0 (110), and Biph/Anth/Naph = 1:1:1 (111) were chosen. It is found from Table S1 that the above samples have similar loading capacity for CPT, which increases with the increasing amount of dye molecules. For example, the decrease in TEOS/Biph ratio from 10 to 1 leads to the improved loading amount from 37 to 50 mg/g of NP, which is much improved compared with the previous report.[17] However, too much introduction of fluorophore (TEOS/Biph = 0.1) improves the hydrophobicity of PMO NP, which is disadvantageous for the bioapplication. Furthermore, the drug release performances of samples (100), (110), and (111) were also compared. As found from the inset in Figure 3A, the releasing rate follows the order

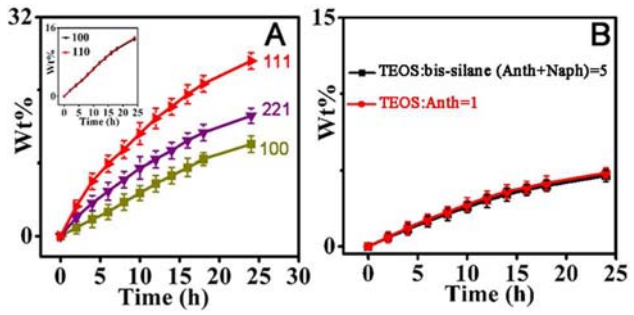

Figure 3. (A) Asynchronous release of CPT from samples (100), (221), and (111). Inset: release of CPT from samples (100) and (110). (B) Synchronous release of DOX and CPT from samples prepared at TEOS/bis-silane (Anth/Naph = 1:5) = 5 and TEOS/Anth = 1.

of (111) > (100) ≈ (110) within 24 h. Since all of these NPs have similar pore size and are prepared at a fixed TEOS/bis-silane ratio, the variable drug releasing performance should be ascribed to the different types of fluorophores inside the framework. Actually, the above tunable retention ability of PMO for CPT is governed by the introduction amount of fluorophore and their polarities, which follows the order of Naph > Anth ≈ Biph. The release rate can be more finely tuned in an asynchronous way by varying the ratio between fluorophores as found from sample (221), which shows a slower release rate than sample (111) but a faster release rate than sample (100).

The above studies on the controlled release of anticancer drug by using CPT as an example clearly indicate that the drug releasing performance of PMO NP can be well correlated with its color, which illustrate the fine adjustability of these NPs as drug carrier. Such kind of colorful NPs provide multiplex options for the synchronous or asynchronous release of different drugs when used as carriers. For some disease therapy, the combinational drug administration is widely used, where the appropriate releasing rates of different drugs are extremely crucial for the achievement of good curing effect. Here, we adopted Doxorubicin hydrochloride (DOX), a generally used substitution drug that is often jointly used with other anticancer drugs, to study the synchronous release performance of the above colorful PMO NPs. Figure S12 indicates that PMO NP prepared at TEOS/Biph = 10 shows completely different releasing rate of CPT (13.3%) and DOX (1%) within 24 h. DOX is positively charged and more hydrophobic than CPT. Therefore, its much lower releasing rate should be ascribed to the joint effects of the hydrophobic fluorophore and negatively charged pore surface covered with hydroxyls. However, the release rates of DOX and CPT can be regulated to be synchronous despite their apparently different properties by carefully tuning the amount and type of fluorophores. As seen from Figure 3B, DOX and CPT show similar release rate in samples prepared at TEOS/bis-silane (Anth/Naph = 1:5) = 5 and TEOS/Anth = 1, respectively, which can emit different colors by a 405 nm argon-ion laser excitation and can be simultaneously observed by the confocal fluorescence microscopy (Figure S13). The improved DOX release rate should be attributed to the dual effects of the decreased amount of surface silanols due to the introduction of more fluorophore and the increased amount of hydrophilic Naph. The above anticancer drugs used for cancer therapy should be released in a synchronous way. However, if the anticancerogen and analgesic drugs are combined, an asynchronous release is better, which should be released in the faster and slower ways, respectively. Therefore, we adopted ibuprofen (IBU), an analgesic drug, for the study of differential release with CPT, which can also be successfully achieved by carefully choosing different colored samples with different hydrophobicity as carriers (Figure S17).

In consideration of the good monodispersity and hydrophilicity of our PMO NP, studies on the cellular uptake efficiency were carried out on HeLa cell lines (5 mL of 50 μg/mL PMO solution). Figure 4 clearly shows that sample (011)

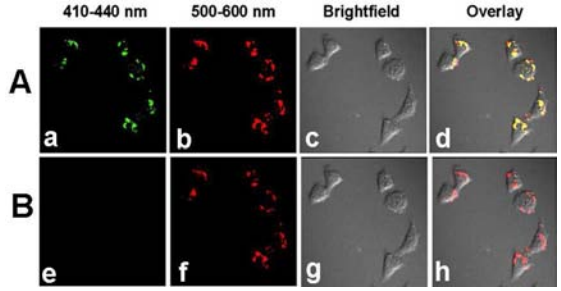

Figure 4. Confocal fluorescence images of living HeLa cells incubated with 50 μg/mL of (011) at 37 °C for 3 h. A and B were acquired under 405 and 488 nm argon-ion laser excitation.

can enter into the cell cytoplasm as a bioimaging reagent, which is further verified by 3-D luminescence images (Figure S14) and the quantitative analysis of the luminescence intensity by flow cytometry (Figure S15). The internalized silicon concentration is 2.8 pg/cell determined by ICP-OES. It is found that only the emission of Naph can be observed (Figure 4B) using the excitation wavelength of Naph at 488 nm. However, two emissions attributed to Anth and Naph can be simultaneously observed from different channels using the excitation wavelength of Anth at 405 nm (Figure 4A) due to the formation of FRET. By varying the ratio between different fluorophores, a colorful bioimaging system benefited from FRET should be obtained. Moreover, the cell viability evaluated using MTT assays (Figure S16) indicates that no obvious growth inhibition is present when the NP concentration is below 10 μg/mL and about 80% cells still survive when the NP concentration increases to 100 μg/mL, which indicate the good

dx.doi.org/10.1021/ja301691j | J. Am. Chem. Soc. 2012, 134, 8746−8749

biocompatibility of PMO NP. The above results well illustrate the multifunctionalities of our colorful PMO NP as the fluorescently traceable drug carrier and bioimaging agent.

In conclusion, we report the first synthesis of multicolorful PMO NP by a single-wavelength excitation with variable surface polarity. Such a kind of composite can be used not only for multiplexed bioimaging, but also as a multifluorescently drug carrier with continuously tunable releasing performance. The synchronous or asynchronous release of different drugs can be successfully achieved by simply choosing NP with different colors. This system provides a good platform for the simultaneous monitoring of drug transports with multiple routes.

■ ASSOCIATED CONTENT

Supporting Information

Experimental details for the synthesis of bis-silanes, PMO NPs, the loading and release of drug, the uptake of NPs into HeLa cells and characterizations including XRD, SEM, and N_2 adsorption−desorption isotherms. This material is available free of charge via the Internet at http://pubs.acs.org.

■ AUTHOR INFORMATION

Corresponding Author

wlz@ecust.edu.cn; jlzhang@ecust.edu.cn

Notes

The authors declare no competing financial interest.

■ ACKNOWLEDGMENTS

This work was supported by National Nature Science Foundation of China (21007016), the Research Fund for the Doctoral Program of Higher Education (20070251006), Science and Technology Commission of Shanghai Municipality (11142201100, 10520709900), and the Fundamental Research Funds for the Central Universities.

■ REFERENCES

(1) Liong, M.; Lu, J.; Kovochich, M.; Xia, T.; Ruehm, S. G.; Nel, A. E.; Tamanoi, F.; Zink, J. I. *ACS Nano* **2008**, *2*, 889.
(2) Lu, J.; Liong, M.; Li, Z.; Zink, J. I.; Tamanoi, F. *Small* **2010**, *6*, 1794.
(3) Lee, J. E.; Lee, N. Y.; Kim, T.; Kim, J. Y.; Hyeon, T. *Acc. Chem. Res.* **2011**, *44*, 893.
(4) Kim, J.; Kim, H.; Lee, N.; Kim, T.; Kim, H.; Yu, T.; Song, I.; Moon, W.; Hyeon, T. *Angew. Chem., Int. Ed.* **2008**, *47*, 8438.
(5) Kim, J.; Lee, J. E.; Lee, J.; Yu, J. H.; Kim, B. C.; An, K.; Hwang, Y.; Shin, C.-H.; Park, J. G.; Kim, J.; Hyeon, T. *J. Am. Chem. Soc.* **2006**, *128*, 688.
(6) Suteewong, T.; Sai, H.; Cohen, R.; Wang, S.; Bradbur, M.; Baird, B.; Gruner, S. M.; Wiesner, U. *J. Am. Chem. Soc.* **2011**, *133*, 172.
(7) Chen, Y.; Chen, H. R.; Zhang, S. J.; Chen, F.; Zhang, L. X.; Zhang, J. M.; Zhu, M.; Wu, H. X.; Guo, L. M.; Feng, J. W.; Shi, J. L. *Adv. Funct. Mater.* **2011**, *21*, 270.
(8) Cheng, S. H.; Lee, C. H.; Chen, M. C.; Souris, J. S.; Tseng, F. G.; Yang, C. S.; Mou, C. Y.; Chen, C. T.; Lo, L. W. *J. Mater. Chem.* **2010**, *20*, 6149.
(9) Lei, J. Y.; Wang, L. Z.; Zhang, J. L. *ACS Nano* **2011**, *5*, 3447.
(10) Wang, L.; Tan, W. H. *Nano Lett.* **2005**, *6*, 84.
(11) Trewyn, B. G.; Slowing, I. I.; Giri, S.; Chen, H. T.; Lin, V. S. Y. *Acc. Chem. Res.* **2007**, *40*, 846.
(12) Hoffmann, F.; Cornelius, M.; Morell, J.; Fröba, M. *Angew. Chem., Int. Ed.* **2006**, *45*, 3216.
(13) Kobler, J.; Möller, K.; Bein, T. *ACS Nano* **2008**, *2*, 791.
(14) Asefa, T.; MacLachan, M. J.; Coombs, N.; Ozin, G. A. *Nature* **1999**, *402*, 867.
(15) Inagaki, S.; Guan, S.; Ohsuna, T.; Terasaki, O. *Nature* **2002**, *416*, 304.
(16) Mizoshita, N.; Tani, T.; Inagaki, S. *Chem. Soc. Rev.* **2011**, *40*, 789.
(17) Lu, J.; Liong, M.; Zink, J. I.; Tamanoi, F. *Small* **2007**, *3*, 1341.